Biogeosciences
Discussions

Open Access

Evolution of ^{231}Pa and ^{230}Th in overflow waters of the North Atlantic

Feifei Deng[1], Gideon M Henderson[1], Maxi Castrillejo[2,3], and Fiz F. Perez[4]

[1]Department of Earth Sciences, University of Oxford, South Parks Road, Oxford, OX13AN, UK.

[2]LaboraLaboratory of Ion Beam Physics, ETH-Zurich, Otto Stern Weg 5, Zurich, 8093, Switzerland

[3]Institut de Ciència i Tecnologia Ambientals & Departament de Física, Universitat Autònoma de Barcelona, Bellaterra, 08193, Spain

[4]Departamento de Oceanografia Instituto Investigaciones Marinas (CSIC), Eduardo Cabello 6, E36208 Vigo, Spain.

Correspondence to: Feifei Deng (feifei.deng@earth.ox.ac.uk)

Abstract. Many paleoceanographic studies have sought to use the ^{231}Pa/^{230}Th ratio as a proxy for deep ocean circulation rates in the North Atlantic. As yet, however, no study has fully assessed the concentration of, or controls on, ^{230}Th and ^{231}Pa in waters immediately following ventilation at the start of Atlantic meridional overturning. To that end, full water-column ^{231}Pa and ^{230}Th concentrations were measured along the GEOVIDE section, sampling a range of young North Atlantic deep waters. Th-230 and ^{231}Pa concentrations in the water column are lower than those observed further south in the Atlantic, ranging between 0.004 and 0.738 dpm/1000l, and between 0.023 and 0.295 dpm/1000l, respectively. Both ^{230}Th and ^{231}Pa profiles generally increase with water depth from surface to deep water, followed by decrease near the seafloor, with this feature most pronounced in the Labrador Sea (LA Sea) and Irminger Sea (IR Sea). Analyzing this dataset with Extended Optimum Multi-Parameter (eOMP) Analysis and CFC-based water mass age indicates that the low values of ^{230}Th and ^{231}Pa in water near the seafloor of the LA Sea and IR Sea are related to the young waters present in those regions. This importance of water age is confirmed for ^{230}Th by a strong correlation between ^{230}Th and water mass age (though this relationship is less clear, for ^{231}Pa and ^{231}Pa/^{230}Th ratio). Scavenged ^{231}Pa and ^{230}Th were estimated and compared to their Potential Total concentrations in the water column. The result shows that more ^{230}Th is scavenged (~80%) relative to ^{231}Pa (~40%), consistent with the relatively higher particle-reactivity of ^{230}Th. Enhanced scavenging for both nuclides is demonstrated near the seafloor in young overflow waters. Calculation of meridional transport of ^{230}Th and ^{231}Pa with this new GEOVIDE dataset enables a complete budget for ^{230}Th and ^{231}Pa for the North Atlantic. Results suggest that net transport southward of ^{230}Th and ^{231}Pa across GEOVIDE is smaller than transport further south in the Atlantic, and indicates that the flux to sediment in the North Atlantic is equivalent to 96% of the production of ^{230}Th, and 77% of the production for ^{231}Pa. This result confirms a significantly higher advective loss of ^{231}Pa to the south relative to ^{230}Th and supports the use of ^{231}Pa/^{230}Th to assess meridional transport at a basin scale.

Key words. GEOTRACES; water-column ^{230}Th and ^{231}Pa; water mass ageing; scavenging; meridional transport.

1 Introduction

Several paleoceanographic proxies have been proposed that rely on the ^{231}Pa/^{230}Th ratio in marine sediments. One of these proxies is that ^{231}Pa/^{230}Th may record the rate of deep-water circulation, particularly in the North Atlantic. Both ^{231}Pa and ^{230}Th are generated continuously by decay of uranium in the water column and are rapidly removed, leading to very low

5   concentrations at the surface and increasing concentrations with depth due to reversible scavenging (Nozaki et al., 1981). Advection of surface waters to depth transports the low concentrations into the deep ocean, where they subsequently increase due to scavenging from above at a rate dependant on the residence time of the nuclide. Because ^{231}Pa has a longer residence time than ^{230}Th (~130 years versus ~20 years, Henderson and Anderson, 2003), the concentration of ^{231}Pa increases more slowly and its resulting removal to the seafloor also increases more slowly. This behaviour means that, in

10   basins such as the North Atlantic with vigorous formation and advection of deep-waters, less ^{231}Pa is removed to the sediment than is produced in the water column. Sediments underlying the North Atlantic will therefore have a ^{231}Pa/^{230}Th below the production ratio, with lower ratios caused by stronger advection.

The use of ^{231}Pa/^{230}Th to constrain past North Atlantic overturning was first proposed by Yu et al. (1996) who measured ^{231}Pa/^{230}Th in Holocene and Last Glacial Maximum (LGM) sediments from many cores from the Atlantic and Southern

15   Ocean. They found similar Holocene and LGM values at a basin scale, suggesting broadly similar overturning during the two periods. Later studies have generally relied on a smaller number of cores (e.g. McManus et al. 2004; Gherardi et al. 2009; Roberts et al. 2014), chosen from particular depths to sample important water masses. This approach relies on the systematic evolution of the ^{231}Pa/^{230}Th ratio in each water mass.

Recent water-column measurements of ^{231}Pa and ^{230}Th on GEOTRACES cruises have shed new light on the chemical

20   controls on these isotopes in seawater. These have indicated that there is considerably more net advection of ^{231}Pa than ^{230}Th out of the North Atlantic (Deng et al., 2014), supporting the basin-scale application of ^{231}Pa/^{230}Th as initially pursued (Yu et al. 1996). But these measurements have also suggested that there is no simple relationship between increasing ^{231}Pa/^{230}Th and age of water, as would be expected if the ^{231}Pa/^{230}Th at single cores is to be interpreted as reflecting the rate of ventilation (e.g. Deng et al., 2014).

25   One important constraint on understanding ^{231}Pa/^{230}Th is to learn about the controls on these isotopes as deep waters form and enter the deep Atlantic. Some measurements have placed initial constraints on ^{231}Pa and ^{230}Th values in young North Atlantic deep waters (e.g. Moran et al., 1997, 2002; Rutgers van der Loeff and Berger, 1993), but there has not yet been a systematic study of the composition of waters in the far north Atlantic. The GEOVIDE cruise allowed waters to be collected for such a study, along a line where significant other data are available, both from that cruise and previous occupations of

30   OVIDE. GEOVIDE provided an ideal opportunity to understand ^{231}Pa and ^{230}Th at the start of the ocean meridional overturning circulation.

2 Sampling strategies and Analytical methods

Seawater samples were collected during the GEOVIDE cruise aboard R/V Pourquoi Pas? from 15 May to 30 June, 2014 as part of GEOTRACES Section GA01. The cruise sampled four regions in the North Atlantic between 40°-60°N: Labrador Sea (LA Sea), Irminger Sea (IR Sea), Iceland Basin (IC Basin), and Western European Basin (WE Basin) (Fig. 1).

5 Full-depth water-column ^{231}Pa and ^{230}Th for this study were collected from 11 stations (Fig. 1). Sampling followed the procedure suggested by GEOTRACES intercalibration work (Anderson et al., 2012). Briefly, seawater samples of 5 Litres were directly filtered from Niskin bottles mounted on the Stainless Steel CTD Rosette through AcroPak^{TM} capsules with Supor$^{®}$ Membrane (0.45 μm pore size). Filtered seawater samples were collected into acid cleaned HDPE plastic bottles, and sealed with a screw cap and Parafilm to reduce evaporation and contamination. Samples were then double bagged for

10 storage in boxes for transport back to the shore-based lab for analysis.

Once returned to the laboratory in Oxford, samples were weighed and then acidified with quartz distilled concentrated HCl to pH ~1.7, shaken and left for at least four days to ensure that Pa and Th was desorbed from the walls of the bottle. A mixed ^{229}Th-^{236}U spike and a ^{233}Pa spike were then added to each sample. The ^{233}Pa spike was freshly made by milking from ^{237}Np (following Regelous et al., 2004) and calibrated against a known ^{236}U solution after complete decay of ^{233}Pa to ^{233}U (i.e.

15 several months after spike production) (Robinson et al., 2004). 50 mg of pure Fe as a chloride solution was also added to each water sample. Samples were left overnight to allow for spike equilibrium after which the pH was raised to ~8.5 using distilled NH$_4$OH to co-precipitate the actinides with insoluble Fe-oxyhydroxides. At least 48 hours were allowed for scavenging of the actinides onto Fe-oxyhydroxides. The precipitate was centrifuged and rinsed, and Th, Pa and U were separated using anion exchange chromatography following Thomas et al., 2006.

20 After chemical separation, Pa and Th were measured on a Nu instrument MC-ICP-MS (Multi Collector-Inductively Coupled Plasma-Mass Spectrometry) at the University of Oxford. Mass discrimination and ion-counter gain were assessed with the measurement of a U standard, CRM-145 U, before each sample measurement. Use of a U standard for this purpose minimises memory problems that might be caused by use of a Th or Pa standard (Thomas et al., 2006). Measurements were also made 0.5 mass units either side of masses of interest to allow accurate correction for the effect of abundance sensitivity

25 on small ^{231}Pa and ^{230}Th beams, and a correction for a small ^{232}ThH interference on the ^{233}Pa beam is made from assessment of the hydride formation rate on a ^{232}Th standard. Concentrations of ^{231}Pa, ^{230}Th together with ^{232}Th were obtained from the precise MC-ICP-MS measurement of ^{231}Pa/^{233}Pa, ^{230}Th/^{229}Th, and ^{232}Th/^{229}Th ratios together with well-calibrated concentrations of ^{233}Pa, and ^{229}Th-^{236}U spikes.

Chemistry blanks were assessed by conducting the complete chemical procedure on ~100 ml of Milli-Q water with each

30 batch of samples. Based on six blank measurements, the average blanks for dissolved ^{231}Pa, ^{230}Th and ^{232}Th are 0.21±0.14 fg, 1.59±0.60 fg and 5.13±1.47 pg, respectively (uncertainties are 2 standard errors). Blank contributions account for 2-22%, 2-26%, and 0.2-16% of the dissolved ^{231}Pa, ^{230}Th and ^{232}Th respectively (with the higher values being for surface samples due to their low concentrations).

3 Results

Measured ^{230}Th and ^{231}Pa concentrations were corrected for blanks, ingrowth from U in seawater since the time of collection, and detrital U-supported ^{230}Th and ^{231}Pa concentrations. Measured and corrected concentrations of ^{230}Th, ^{231}Pa, and ^{232}Th, along with details of corrections, are provided in the Supplemental Information S1. Although analysis was conducted in

5   terms of fg/kg, results are converted to dpm/1000l for ease of comparison with previous work. This conversion assumes that the density of seawater was uniformly 1.025 g/cm^3 and half-lives for ^{231}Pa, ^{230}Th and ^{232}Th of 32,760 yr, 75,584 yr and 1.405×10^{10} yr, respectively (Robert et al., 1969; Cheng et al., 2013; Holden, 1990). Uncertainties were propagated, including the contribution from sample weighing, spike calibration, impurities in the spikes, blank corrections, and mass spectrometric measurement, and are reported as 2 standard errors (2 s.e.). Average total uncertainties for ^{231}Pa, ^{230}Th and ^{232}Th are ±0.010

10   dpm/1000l, ±0.010 dpm/1000l, and ±0.00018 dpm/1000l, respectively. Vertical profiles showing the results of corrected ^{230}Th and ^{231}Pa concentrations in the water column are plotted by region in Fig. 2.

Th-230 concentrations in the water column range between 0.004 and 0.738 dpm/1000l, and initially generally increase with water depth from surface to deep water. Towards the seafloor, six of the eleven stations show a prominent decrease of ^{230}Th, with this feature most pronounced in the LA and IR Seas.

15   Pa-231 concentrations in the water column range between 0.023 and 0.295 dpm/1000l and also increase with water depth, but less rapidly than ^{230}Th. ^{231}Pa profiles also often exhibit a decrease near the seafloor at stations showing a ^{230}Th decrease. Station 38 at the Reykjanes Ridge distinguishes itself from other ^{231}Pa profiles in that an increase in ^{231}Pa concentrations from low concentrations at 1000 m is observed, continuing towards the bottom.

Observed ^{230}Th and ^{231}Pa values at GEOVIDE are lower than those observed in intercalibrated GEOTRACES data from

20   further south in the Atlantic. Figure 3 compares average depth profiles for GEOVIDE with those from the mid-latitude North Atlantic (GEOTRACES section GA03_w, Hayes et al., 2015) and the South Atlantic (GEOTRACES section GA10, unpublished data by Deng et al. available in the GEOTRACES Intermediate Data Product). A southward increase of both ^{230}Th and ^{231}Pa concentrations is observed below 1000 m.

4 Discussion

25   Early studies of water-column ^{230}Th and ^{231}Pa reported a linear increase of both nuclides with water depth (e.g. Anderson et al., 1983; Nozaki et al., 1981), and introduced a reversible scavenging model with exchange of both nuclides between their dissolved and particulate phases. Later studies observed a deviation of ^{230}Th and ^{231}Pa profiles from this reversible scavenging model, with the expected increase with depth often inverting near the seafloor. Rutgers van der Loeff and Berger (1993) observed that ^{230}Th concentrations decrease in the bottom water in the South Atlantic south of the Antarctic Polar

30   Front and interpreted this as the influence of relatively young bottom water in the region. Okubo et al. (2012) also found decreasing ^{230}Th values near the seafloor in the North Pacific and, in the absence of ventilation in the area, interpreted these

as due to bottom scavenging. Deng et al. (2014) observed low concentrations of both ^{230}Th and ^{231}Pa in near-bottom water coinciding with the presence of the nepheloid layer, and interpreted the low values as a result of enhanced scavenging by resuspended particles in the nepheloid layer.

In this study, recently ventilated overflow waters are sampled at depth, particularly in the Labrador and Irminger Seas. Low values of ^{230}Th and ^{231}Pa near the seafloor might be expected to relate to these young waters, but the effects of scavenging must also be considered.

4.1 Water mass distribution and influence

The presence of multiple water masses sampled by the GEOVIDE Section allows the influence of water mass (and age) on ^{230}Th and ^{231}Pa to be assessed. Extended Optimum Multi-Parameter (eOMP) Analysis (García-Ibáñez et al., 2018) for the GEOVIDE section maps the presence of 10 water-mass end-members in the section (Fig. 4).

This eOMP analysis indicates three recently ventilated waters in the GEOVIDE section:

i. Labrador Sea Water (LSW), which is formed by deep convection (Talley and McCartney, 1982), is the dominant water along the section, extending from 1000 to 2500 m depth in the east and from surface to 3500 m in the west of the section.

ii. Iceland–Scotland Overflow Water (ISOW), which is formed in the Norwegian Sea and subsequently entrains overlying warmer and more salty waters. This water mass initially flows along the eastern flank of the Reykjanes Ridge before spreading back northwards, after crossing the Charlie-Gibbs Fracture Zone, into the Irminger and Labrador Seas (Dickson and Brown, 1994; Saunders, 2001). A pronounced layer of this water mass is observed immediately below the LSW, and extends to a water depth as deep as 4000 m west of 20°W.

iii. Denmark Strait Overflow Water (DSOW), which is formed after the Nordic Seas deep waters overflow and entrains Atlantic waters (SPMW and LSW) (Yashayaev and Dickson, 2008) with dense Greenland shelf water cascading down to the DSOW layer in the Irminger Sea (Falina et al., 2012; Olsson et al., 2005; Tanhua et al., 2005). This water occupies the deepest part of the IR and LA Seas.

In the east of the section, deep waters consist of the much older Lower North East Atlantic Deep Water (NEADW$_L$) which is formed with a significant southern component from the Antarctic Bottom Water. A number of other water masses are also observed at shallow depths, including Mediterranean Water, and various Mode Waters.

Some control of water mass on ^{230}Th and ^{231}Pa concentration is evident in nuclide section plots (Fig. 5), particularly relatively low ^{230}Th and ^{231}Pa concentrations in DSOW and high values in the old NEADW. In other places, the impact of water mass is less apparent. The challenge with these nuclides is that they are not conservative tracers of water mass, but evolve significantly during transport and water aging. On the GEOVIDE Section we can analyse this evolution because the ages of the water-masses can be assessed from CFC data.

CFC measurements are not available along the GEOVIDE line, but Paz et al., (2017) determined the CFC-based age along the west of the section (covering WE Basin, IC Basin, and IR Sea) in 2012 (OVIDE/CATARINA cruise). We projected the

CFC-based age along GEOVIDE line using the water mass distributions (Steinfedt personal communication). Using the water mass distribution along GEOVIDE given by Garcia-Ibanez et al. (2018) and the distribution for the same water masses in 2012 (Garcia-Ibañez et al. (2015), we derived CFC-based age measurements for GEOVIDE (Fig. 6; further details in Supplemental Information S2).

5 CFC-based water-mass ages range from ≈10 years, observed in DSOW at the bottom of the LA Sea, to ≈800 years, observed for NEADW at the bottom of the WE Basin. Because this study focuses on understanding controls on ^{231}Pa and ^{230}Th in recently ventilated waters, we omit detailed consideration of the upper 1km in subsequent discussion, and restrict our analysis to water sampled west of 35°W of the section where young waters dominate. A rescaled version of the CFC age section indicates the variation in age of ventilated waters (Fig. 6b). DSOW, occupying the deepest LA and IR Seas, is the

10 youngest water mass in this region, with an average age of ~19 years. ISOW and LSW are slightly older, with ages ranging from 26 to 45 years and 32 to 40 years respectively.

4.2 Evolution of ^{230}Th and ^{231}Pa with water age

The presence of recently ventilated deep-waters with constrained CFC ages allows analysis of the rates at which ^{230}Th and ^{231}Pa concentrations increase during transport, and the rates of scavenging of these nuclides. To conduct this analysis, we

15 define five components in the budget of ^{230}Th and ^{231}Pa:

i. Preformed component: The ^{230}Th or ^{231}Pa transported from the surface into the interior. For this analysis, in the absence of measurements for the exact location of deep-water formation, we set the preformed value as the average of concentrations measured in waters <100 m depth for this section to give preformed concentrations of 0.108 dpm/1000l for ^{230}Th and 0.089 dpm/1000l for ^{231}Pa. This preformed ^{230}Th and ^{231}Pa will decrease due to radioactive decay during transport. Although we

20 take this decay into account in the following analysis, it is insignificant given the ages of waters involved and the much longer half-lives of ^{230}Th and ^{231}Pa.

ii. Ingrown component: The ingrown ^{230}Th or ^{231}Pa from radioactive decay of U since the water was last in contact with the surface. This component increases as the water mass ages. The concentration of this component in a water mass of age t can be calculated as:

25
$$^{230}Th_{Ingrown} = {}^{234}U \times (1 - e^{-\lambda_{230}t}) \qquad (4.1)$$

$$^{231}Pa_{Ingrown} = {}^{235}U \times (1 - e^{-\lambda_{231}t}) \qquad (4.2)$$

where ^{230}Th$_{Ingrown}$ and ^{231}Pa$_{Ingrown}$ are the ^{230}Th and ^{231}Pa ingrown from their U parents, respectively; ^{238}U and ^{235}U are activities of ^{234}U, and ^{235}U in seawater (2801.4 dpm/1000l and 112.2 dpm/1000l, respectively); λ_{230} and λ_{231} are decay constants of ^{230}Th and ^{231}Pa (9.17 ×10^{-6} yr^{-1} and 2.12×10^{-5} yr^{-1}, respectively).

30 *iii. Potential Total component*: The ^{230}Th and ^{231}Pa expected in the water due to the combination of preformed and ingrown components, if there were no removal by scavenging.

iv. Observed component: The ^{230}Th and ^{231}Pa observed in the water column, i.e. dissolved ^{230}Th and ^{231}Pa measured in this study (after correction for detritus and ingrowth from U since sample collection).

v. Scavenged component: The net ^{230}Th or ^{231}Pa removed from the water since it left the surface due to scavenging. For each depth, this component is the net of nuclide added from above by settling particles, and the removal downwards by scavenging.

These components are related to each other as follows:

$$Preformed\ + Ingrown = Potential\ Total\ ^{230}Th\ \left(or\ ^{231}Pa\right) =\ Observed + Scavenged \qquad (4.3)$$

The difference between the Potential Total and the Observed concentration of ^{230}Th (or ^{231}Pa), therefore provides a measure of the amount of nuclide scavenged since the water left the surface (Fig. 7).

We examine the evolution of both the observed and scavenged components of ^{230}Th and ^{231}Pa with water mass age (Fig. 8). Both ^{230}Th and ^{231}Pa show an increase in observed concentration with age of water, with the increase for ^{230}Th much more regular than for ^{231}Pa. This strong ^{230}Th relationship, regardless of depth of the sample (Fig. 8a), indicates a primary control of water-mass age on the increase of ^{230}Th in these younger waters.

For ^{230}Th, the rate of increase with age (i.e. slope in Fig. 8a) indicates that about one quarter of the ^{230}Th formed from U decay remains in the water, with the other three quarters being removed by scavenging. This ratio is consistent with the average ^{230}Th for these waters, which requires that about three times more ^{230}Th has been removed by scavenging. The scatter between ^{231}Pa and age (Fig. 8c) precludes the use of the slope to assess the relative proportion of scavenged ^{231}Pa, but the average values (Fig. 8c, 8d) indicate that about half of the ^{231}Pa remains in the water, while half is removed by scavenging. The relative behaviour of ^{230}Th and ^{231}Pa is consistent with previous expectations, with a higher fraction of scavenging of ^{230}Th than ^{231}Pa.

The hypothesis that ^{231}Pa/^{230}Th ratios increase as water mass ages forms the foundation of using ^{231}Pa/^{230}Th in discrete cores as a deep-ocean circulation tracer in paleoceanography (e.g. McManus et al. 2004). For these young waters, however, there is no clear relationship between observed ^{231}Pa/^{230}Th and age (Fig. 8e), nor between the ^{231}Pa/^{230}Th value scavenged to the sediment and age (Fig. 8f). In the next section, we investigate the possible controls on this ratio in these younger waters.

4.3 The importance of Preformed ^{230}Th and ^{231}Pa in young waters

To assess the controls on ^{230}Th, ^{231}Pa, and particularly the resulting ^{231}Pa/^{230}Th ratio, we apply a simple scavenging-mixing model following Moran et al. (1997). This model was first created to assess the evolution of ^{230}Th in a 1D water column as it ages following ventilation. Here we adapt it by modelling the nuclide evolution with age for each depth, and by also modelling ^{231}Pa. This makes the assumption that waters have remained at the same depth since ventilation which, though not correct in detail, still allows the model to provide insights about controls on these nuclides.

The model requires values for four parameters: particle settling speed (S), suspended particle concentration (SPM), and distribution coefficients for ^{230}Th (K_d^{Th}) and ^{231}Pa (K_d^{Pa}). We select these parameters to give a good fit to the ^{230}Th and ^{231}Pa observations at Station 1 and 13 on the east of the section (i.e. those with older waters) and use these values to interpret the younger waters to the west. Best fits to the Station 1 and 13 data suggested S = 800 m/yr; SPM = 25 µg/l; K_d^{Th} =1.1×10^7

5   ml/g; and K_d^{Pa} = 2.0×10^6 ml/g (the first three of these are close to those of Moran et al. 1997). A fuller description of the model is given in Supplemental Information S3.

We run the model twice, once with a preformed component (C_{pre}) equal to the nuclide concentrations observed in the upper 100 m of the GEOVIDE section (as in 4.2 above), and once with C_{pre} = 0 for both nuclides. For both cases, the modelled evolution with age of nuclide concentrations at 2000 m and 3500 m is plotted in Fig. 9, and compared to data.

10   As expected, modeled ^{230}Th and ^{231}Pa concentrations increase with age, with deeper waters having higher concentrations and ^{230}Th increasing more rapidly initially (Fig. 9). The fit of the model to observations in young waters from GEOVIDE is improved in the model run with zero preformed nuclide, particularly for ^{230}Th. This is surprising, given that surface-water ^{230}Th and ^{231}Pa values are generally non-zero, and typically close to the value observed in the GEOVIDE surface waters (e.g. Henderson and Anderson, 2003). For ^{230}Th in young deep waters, even the model with zero preformed nuclide

15   overestimates the observed value, possibly indicating additional scavenging from these waters close to the seafloor.

The most striking effect of changing the assumed preformed values in the model is on ^{231}Pa/^{230}Th (Fig. 9c). When preformed values are set at zero, ^{231}Pa/^{230}Th ratios increase as water age increases, but when set at the average surface value from GEOVIDE, ^{231}Pa/^{230}Th ratios initially decrease and are then approximately constant. This indicates that knowledge of the nuclide concentration at the site of deep-water formation is critical to understanding the early evolution of ^{231}Pa/^{230}Th in

20   waters and their underlying sediments.

4.4 Scavenging of ^{230}Th and ^{231}Pa

Knowledge of the CFC ages of the waters analysed on the GEOVIDE cruise allow an assessment of the scavenging rates of ^{230}Th and ^{231}Pa. To do so, we compare the Scavenged component to the Potential Total component (as defined in Section 4.2).

25   The percentage of the Scavenged component relative to the Potential Total component is higher for ^{230}Th, at an average of 80%, than for ^{231}Pa at an average of 40% (Fig. 10), consistent with the relatively higher particle-reactivity of ^{230}Th. For both nuclides, there is higher fraction of scavenging in samples from near the seafloor, particularly those in from DSOW in the deepest LA Sea. Bottom scavenging has been indicated in previous studies (e.g. Okubo et al. 2012, Deng et al. 2014) but this study indicates that this enhanced nuclide scavenging occurs even in the very young overflow waters at the start of the

30   meridional circulation.

4.5 Meridional transport of ^{230}Th and ^{231}Pa in the North Atlantic

Previous calculations have indicated removal of ^{230}Th and ^{231}Pa from the North Atlantic by meridional transport southward. Deng et al. (2014) calculated net southward transport of 6% of the ^{230}Th and 33% of ^{231}Pa, relative to production of these nuclides in the water column. That calculation, however, did not provide a complete budget for ^{230}Th and ^{231}Pa for the

5   North Atlantic because observations at the time did not constrain input of these nuclides from the north. Data in this study allow this calculation, and therefore a more complete budget for the modern North Atlantic.

García-Ibáñez et al. (2018) calculated volume transports for the Portugal to Greenland section of the GEOVIDE section by combining the water mass fractions from eOMP analysis with the absolute geostrophic velocity field calculated using inverse model constrained by Doppler current profiler velocity measurements (Zunino et al., 2017). They defined between

10   northward flowing upper, and southward flowing lower limbs of the AMOC at isopycnal $\sigma_1 = 32.15$ kg/m^3, with $+18.7 \pm 2.4$ Sv and -17.6 ± 3.0 Sv flow across the section above and below this value (positive value indicates northward transport). With average ^{230}Th and ^{231}Pa concentrations in the upper limb of 0.098 and 0.082 dpm/1000l respectively, northward transport of ^{230}Th is 1.83×10^6 and of ^{231}Pa is 1.53×10^6 dpm/s. Average ^{230}Th and ^{231}Pa concentrations in the lower limb are 0.22 and 0.15 dpm/1000l, respectively, indicating transports of ^{230}Th and ^{231}Pa are -3.87×10^6 and -2.64×10^6 dpm/s,

15   respectively.

Net transport of ^{230}Th and ^{231}Pa across GEOVIDE is therefore to the south, and supplies 2.04×10^6 dpm/s ^{230}Th and 1.11×10^6 dpm/s ^{231}Pa to the North Atlantic (Fig. 11). This is a smaller net transport than further south in the Atlantic (Fig. 11), due to the lower ^{230}Th and ^{231}Pa concentrations in the water column close of the site of deep-water formation.

The budget for these nuclides for the North Atlantic consists of: production in the water column; addition by advection from

20   the North; loss by advection to the South and removal to the sediment. The data from this study allows this budget to be fully assessed, and indicates that the flux to the sediment is equivalent to 96% of the production of ^{230}Th, and 77% of the production for ^{231}Pa. For both nuclides, these fluxes are higher than in previous calculations (Deng et al. 2014) which ignored advective fluxes from the North. There is, however, still a significantly higher advective loss of ^{231}Pa relative to ^{230}Th. At a basin scale, therefore, ^{231}Pa/^{230}Th in the sediment must be lower than the production ratio. This lower value is

25   generated by the meridional transport of the North Atlantic, and likely to be sensitive to changes in this transport. Use of ^{231}Pa/^{230}Th to assess meridional transport at a basin scale, as initially proposed by Yu et. al (1996), is therefore still supported by the full modern North Atlantic budget for these nuclides.

5 Conclusion

Measurement of ^{230}Th and ^{231}Pa in waters from GEOVIDE show some control of water mass on ^{230}Th and ^{231}Pa

30   concentrations, particularly low concentrations in DSOW and high values in the old NEADW. There is, however, no close mapping of nuclide concentration to water mass.

With the availability of CFC ages on this section, the evolution of ^{230}Th and ^{231}Pa concentration with age is possible. A systematic increase of ^{230}Th concentration is observed over the first 50 years following ventilation, and a similar though more scattered relationship seen for ^{231}Pa. There is no clear relationship between the ^{231}Pa/^{230}Th ratio and age for these young waters. The evolution of ^{231}Pa/^{230}Th is found from a simple model to be highly dependent on the preformed

5 concentrations for these nuclides, which complicates potential use of ^{231}Pa/^{230}Th in young waters. This analysis of the ^{230}Th and ^{231}Pa concentration relative to the age of the water not only demonstrates the influence of water mass aging on ^{231}Pa and ^{230}Th, but also points to the influence of scavenging. Scavenged ^{230}Th is much more extensive that ^{231}Pa, as expected, and enhanced removal of both nuclides is seen immediately above the seafloor, particularly for young waters.

Calculation of meridional transport of ^{230}Th and ^{231}Pa indicates a southward net transport of both nuclides across the

10 GEOVIDE section. This advection is smaller than that further south in the Atlantic as a result of lower ^{230}Th and ^{231}Pa concentrations at GEOVIDE. Calculation of the flux across GEOVIDE allows a more complete budget for the North Atlantic to be constructed. This demonstrates a significantly higher advective loss of ^{231}Pa to the south relative to ^{230}Th demonstrates, with 23% of the ^{231}Pa produced advected southward from the basin (relative to only 4% for ^{230}Th), and continues to support the use of sedimentary ^{231}Pa/^{230}Th measurements at a basin scale to constrain overturning circulation.

15 **Acknowledgements**

References

Anderson, R. F., Bacon, M. P. and Brewer, P. G.: Removal of ^{230}Th and ^{231}Pa from the open ocean, Earth Planet. Sci. Lett., 62(1), 7–23, doi:https://doi.org/10.1016/0012-821X(83)90067-5, 1983.

30 Anderson, R. F., Fleisher, M. Q., Robinson, L. F., Edwards, R. L., Hoff, J. A., Moran, S. B., van der Loeff, M. R., Thomas,

A. L., Roy-Barman, M. and Francois, R.: GEOTRACES intercalibration of [230]Th, [232]Th, [231]Pa, and prospects: For [10]Be, Limnol. Oceanogr. Methods, 10, 179–213, doi:10.4319/lom.2012.10.179, 2012.

Cheng, H., Edwards, L.R., Shen, C.-C., Polyak, V. J., Asmerom, Y., Woodhead, J., Hellstrom, J., Wang, Y., Kong, X., Spötl, C., Wang, X. and Calvin, A. E.: Improvements in [230]Th dating, [230]Th and [234]U half-life values, and U–Th isotopic measurements by multi-collector inductively coupled plasma mass spectrometry, Earth Planet. Sci. Lett., 371, 82–91, doi:10.1016/j.epsl.2013.04.006, 2013.

Deng, F., Thomas, A. L., Rijkenberg, M. J. A. and Henderson, G. M.: Controls on seawater [231]Pa, [230]Th and [232]Th concentrations along the flow paths of deep waters in the Southwest Atlantic, Earth Planet. Sci. Lett., 390, 93–102, doi:https://doi.org/10.1016/j.epsl.2013.12.038, 2014.

Dickson, R. R. and Brown, J.: The production of North Atlantic Deep Water: Sources, rates, and pathways, J. Geophys. Res. Ocean., 99(C6), 12319–12341, doi:10.1029/94JC00530, 1994.

Falina, A., Sarafanov, A., Mercier, H., Lherminier, P., Sokov, A. and Daniault, N.: On the Cascading of Dense Shelf Waters in the Irminger Sea, J. Phys. Oceanogr., 42(12), 2254–2267, doi:10.1175/JPO-D-12-012.1, 2012.

García-Ibáñez, M. I., Pardo, P. C., Carracedo, L. I., Mercier, H., Lherminier, P., Ríos, A. F. and Pérez, F. F.: Structure, transports and transformations of the water masses in the Atlantic Subpolar Gyre, Prog. Oceanogr., 135, 18–36, doi:https://doi.org/10.1016/j.pocean.2015.03.009, 2015.

García-Ibáñez, M.I., Pérez, F.F., Lherminier, P., Zunino, P., Mercier, H., Tréguer, P.: Water mass distributions and transports for the 2014 GEOVIDE cruise in the North Atlantic. Biogeosciences 15, 2075–2090, https://doi.org/10.5194/bg-15-2075-2018, 2018.

Gherardi, J.M., Labeyrie, L., Nave, S., Francois, R., McManus, J.F., Cortijo, E: Glacial-interglacial circulation changes inferred from [231]Pa/[230]Th sedimentary record in the North Atlantic region, Paleoceanography, 24(2), doi:10.1029/2008PA001696, 2009.

Hayes, C. T., Anderson, R. F., Fleisher, M. Q., Huang, K. F., Robinson, L. F., Lu, Y., Cheng, H., Edwards, R. L. and Moran, S. B.: [230]Th and [231]Pa on GEOTRACES GA03, the U.S. GEOTRACES North Atlantic transect, and implications for modern and paleoceanographic chemical fluxes, Deep. Res. Part II Top. Stud. Oceanogr., 116, 29–41, doi:10.1016/j.dsr2.2014.07.007, 2015.

Henderson, G. M. and Anderson, R. F.: The U-series Toolbox for Paleoceanography, Rev. Mineral. Geochemistry, 52(1), 493–531 [online] Available from: http://dx.doi.org/10.2113/0520493, 2003.

Holden, N.E.: Total half-lives for selected nuclides , Pure Appl. Chem. , 62, 941, doi:10.1351/pac199062050941 , 1990.

McManus, J. F., Francois, R., Gherardi, J.-M., Keigwin, L. D. and Brown-Leger, S.: Collapse and rapid resumption of Atlantic meridional circulation linked to deglacial climate changes, Nature, 428, 834,[online] Available from: http://dx.doi.org/10.1038/nature02494, 2004.

Moran, S. B., Charette, M. A., Hoff, J. A. and Edwards, R. L.: Distribution Of Th-230 In the Labrador Sea and Its Relation to Ventilation, Earth Planet. Sci. Lett., 150, 151–160, 1997.

Moran, S. B., Shen, C., Edmonds, H. N., Weinstein, S. E., Smith, J. N. and Edwards, R. L.: Dissolved and particulate ^{231}Pa and ^{230}Th in the Atlantic Ocean : constraints on intermediate / deep water age , boundary scavenging , and ^{231}Pa / ^{230}Th fractionation, Earth Planet. Sci. Lett., 203, 999–1014, 2002.

Nozaki, Y., Horibe, Y. and Tsubota, H.: The water column distributions of thorium isotopes in the western North Pacific, Earth Planet. Sci. Lett., 54(2), 203–216, doi:https://doi.org/10.1016/0012-821X(81)90004-2, 1981.

Okubo, A., Obata, H., Gamo, T. and Yamada, M.: ^{230}Th and ^{232}Th distributions in mid-latitudes of the North Pacific Ocean: Effect of bottom scavenging, Earth Planet. Sci. Lett., 339–340, 139–150, doi:10.1016/j.epsl.2012.05.012, 2012.

Olsson, K. A., Jeansson, E., Anderson, L. G., Hansen, B., Eldevik, T., Kristiansen, R., Messias, M.-J., Johannessen, T. and Watson, A. J.: Intermediate water from the Greenland Sea in the Faroe Bank Channel: spreading of released sulphur hexafluoride, Deep Sea Res. Part I Oceanogr. Res. Pap., 52(2), 279–294, doi:https://doi.org/10.1016/j.dsr.2004.09.009, 2005.

Paz, M., García-Ibáñez Maribel, I., Steinfeldt, R., Ríos Aida, F. and Pérez Fiz, F.: Ventilation versus biology: What is the controlling mechanism of nitrous oxide distribution in the North Atlantic?, Global Biogeochem. Cycles, 31(4), 745–760, doi:10.1002/2016GB005507, 2017.

Regelous, M., Turner, S., Elliott, T., Rostami, K. and Hawkesworth, C.: Measurement of Femtogram Quantities of Protactinium in Silicate Rock Samples by Multicollector Inductively Coupled Plasma Mass Spectrometry, Anal. Chem., 76(1), doi:10.1021/ac702316r, 2004.

Robert, J., Miranda, C.F. and Muxart, R., 1969. Mesure de la periode du protactinium-231 par microcalorimetrie. Radiochimica Acta 11, 104-108.

Roberts, N.L., McManus, J.F., Piotrowski, A.M., McCave, I.N.: Advection and scavenging controls of Pa/Th in the northern NE Atlantic, Paleoceanography, 29(6), 668–679, doi:10.1002/2014PA002633, 2014.

Robinson, L. F., Belshaw, N. S. and Henderson, G. M.: U and Th concentrations and isotope ratios in modern carbonates and waters from the Bahamas, Geochim. Cosmochim. Acta, 68(8), 1777–1789, doi:https://doi.org/10.1016/j.gca.2003.10.005, 2004.

Rutgers van der Loeff, M. M. and Berger, G. W.: Scavenging of ^{230}Th and ^{231}Pa near the antarctic polar front in the South Atlantic, Deep Sea Res. Part I Oceanogr. Res. Pap., 40(2), 339–357, doi:https://doi.org/10.1016/0967-0637(93)90007-P, 1993.

Saunders, P. M.: The dense northern overflows, in *Ocean Circulation and Climate*, edited by G. Siedler, J. Church, and J. Gould, pp. 401–417, Academic, New York, 2001.

Talley, L. D. and McCartney, M. S.: Distribution and Circulation of Labrador Sea Water, J. Phys. Oceanogr., 12(11), 1189–1205, doi:10.1175/1520-0485(1982)012<1189:DACOLS>2.0.CO;2, 1982.

Tanhua, T., Olsson, K. A. and Jeansson, E.: Formation of Denmark Strait overflow water and its hydro-chemical composition, J. Mar. Syst., 57(3), 264–288, doi:https://doi.org/10.1016/j.jmarsys.2005.05.003, 2005.

Thomas, A. L., Henderson, G. M. and Robinson, L. F.: Interpretation of the ^{231}Pa/^{230}Th paleocirculation proxy: New water-column measurements from the southwest Indian Ocean, Earth Planet. Sci. Lett., 241(3), 493–504,

doi:https://doi.org/10.1016/j.epsl.2005.11.031, 2006.

Yashayaev, I. and Dickson, B.: Transformation and Fate of Overflows in the Northern North Atlantic BT - Arctic–Subarctic Ocean Fluxes: Defining the Role of the Northern Seas in Climate, edited by R. R. Dickson, J. Meincke, and P. Rhines, pp. 505–526, Springer Netherlands, Dordrecht., 2008.

5   Yu, E.-F., Francois, R. and Bacon, M. P.: Similar rates of modern and last-glacial ocean thermohaline circulation inferred from radiochemical data, Nature, 379, 689 [online] Available from: http://dx.doi.org/10.1038/379689a0, 1996.

Zunino, P., Lherminier, P., Mercier, H., Daniault, N., García-Ibáñez, M. I. and Pérez, F. F.: The GEOVIDE cruise in May–June 2014 reveals an intense Meridional Overturning Circulation over a cold and fresh subpolar North Atlantic, Biogeosciences, 14(23), 5323–5342, doi:10.5194/bg-14-5323-2017, 2017.
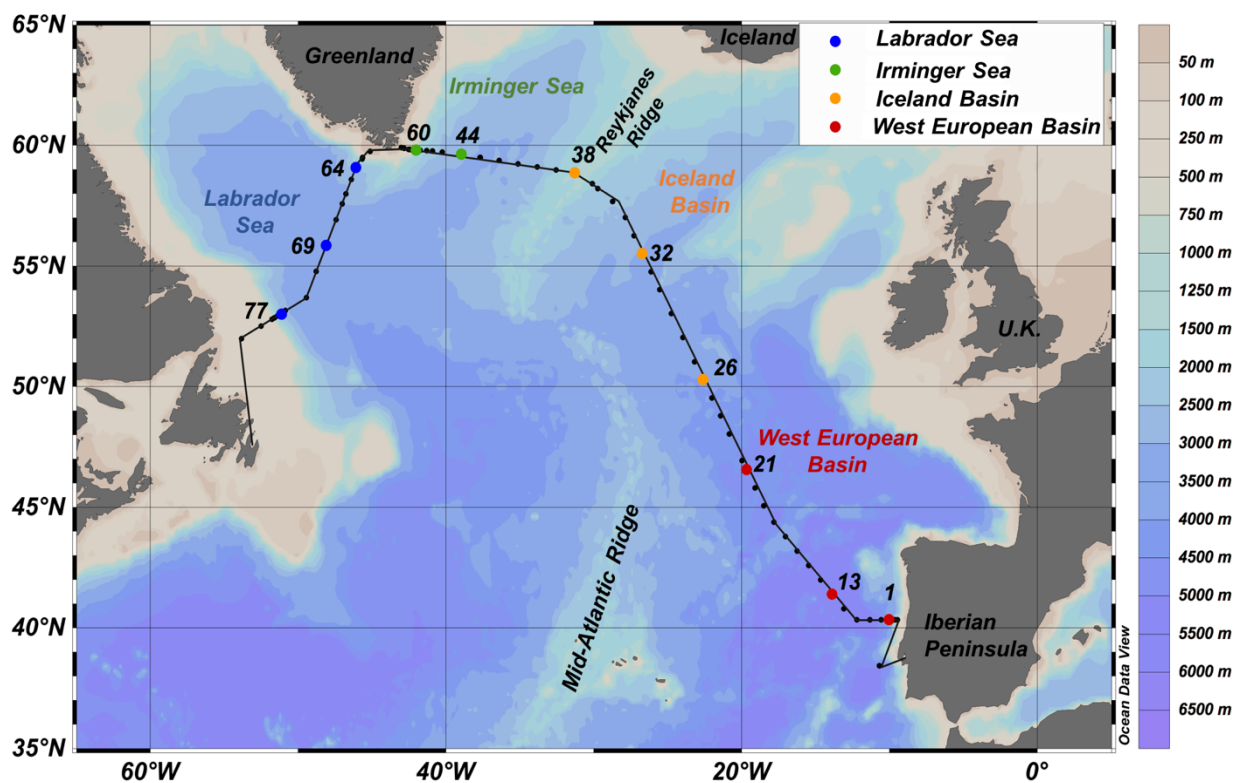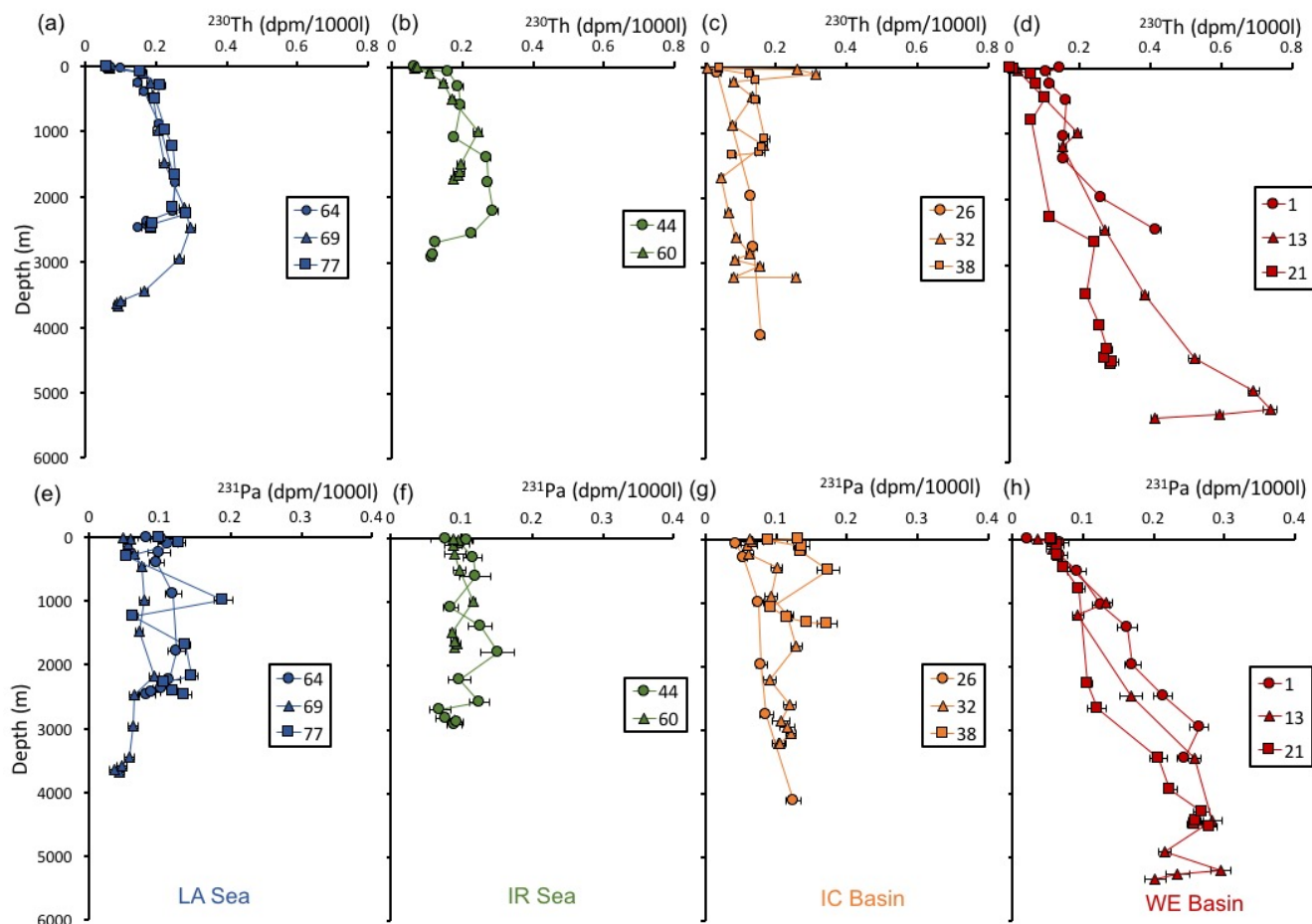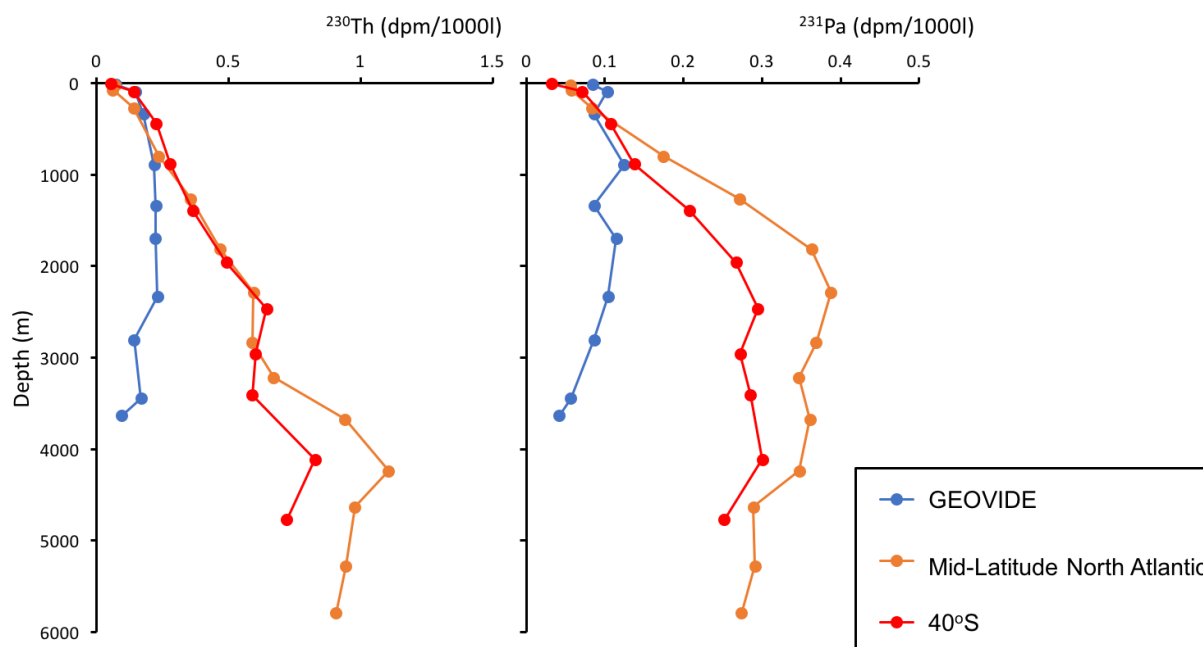
Figure 1: Map showing GEOVIDE cruise track (black line) and station locations (black dots). Sampling locations for water-column ^{231}Pa and ^{230}Th in this study are shown by coloured dots, with colours representing the ocean regions they are located in.

Figure 2: Vertical profiles of ^{230}Th (a-d) and ^{231}Pa (e-h) in the water column along the GEOVIDE section. Colours corresponds to the region (as in Fig. 1). LA = Labrador, IR = Irminger, IC = Iceland, WE = West European). Uncertainties represent 2 standard error (2 s.e.).

Figure 3: Vertical profiles of ^{230}Th and ^{231}Pa from west of the Mid-Atlantic Ridge in high latitude North Atlantic (GEOVIDE), mid-latitude North Atlantic, and 40°S South Atlantic. Data from all stations were sorted by water depth and averages for depth and ^{230}Th and ^{231}Pa concentrations were taken for 0-50 m, 50-100 m, 100- 500 m, and every 500 m interval below.
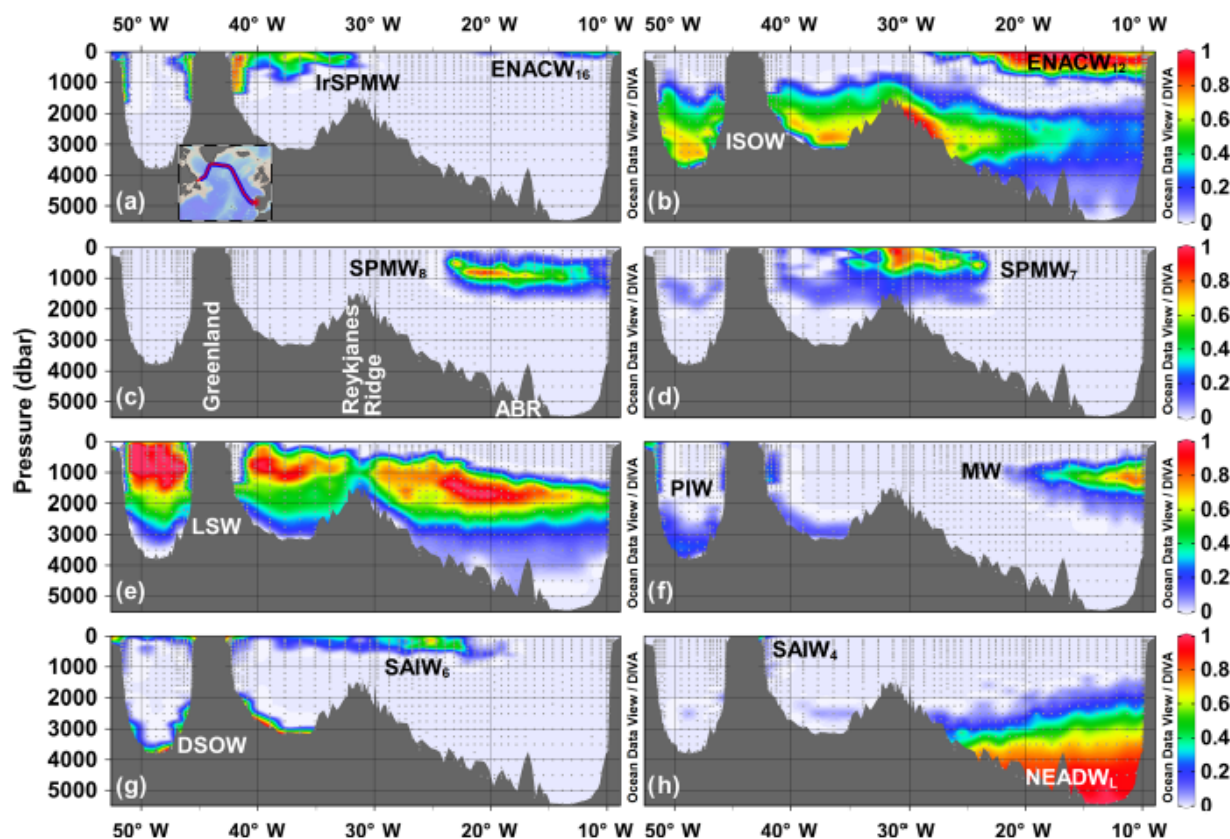
Figure 4: Results of Extended Optimum MultiParameter (eOMP) analysis for the GEOVIDE section (García-Ibáñez et al., 2018).
Colours reflect the fraction of water at each location assigned to the water mass shown in that panel: $ENACW_{16}$ and $ENACW_{12}$ =
East North Atlantic Central Water of 16°C and 12°C; $SPMW_8$, $SPMW_7$, IrSPMW = Subpolar Mode Water of 8°C, 7°C and of the
5 **Irminger Sea; $SAIW_6$ and $SAIW_4$ = Subarctic Intermediate Water of 6°C and 4°C; MW = Mediterranean Water; PIW = Polar**
Intermediate Water; SAIW=Subarctic Intermediate Waters; ISOW=Iceland–Scotland Overflow Water; LSW=Labrador Sea
Water; DSOW: Denmark Strait Overflow Waters; and $NEADW_L$: Lower North East Atlantic Deep Water; ABR= Azores-Biscay
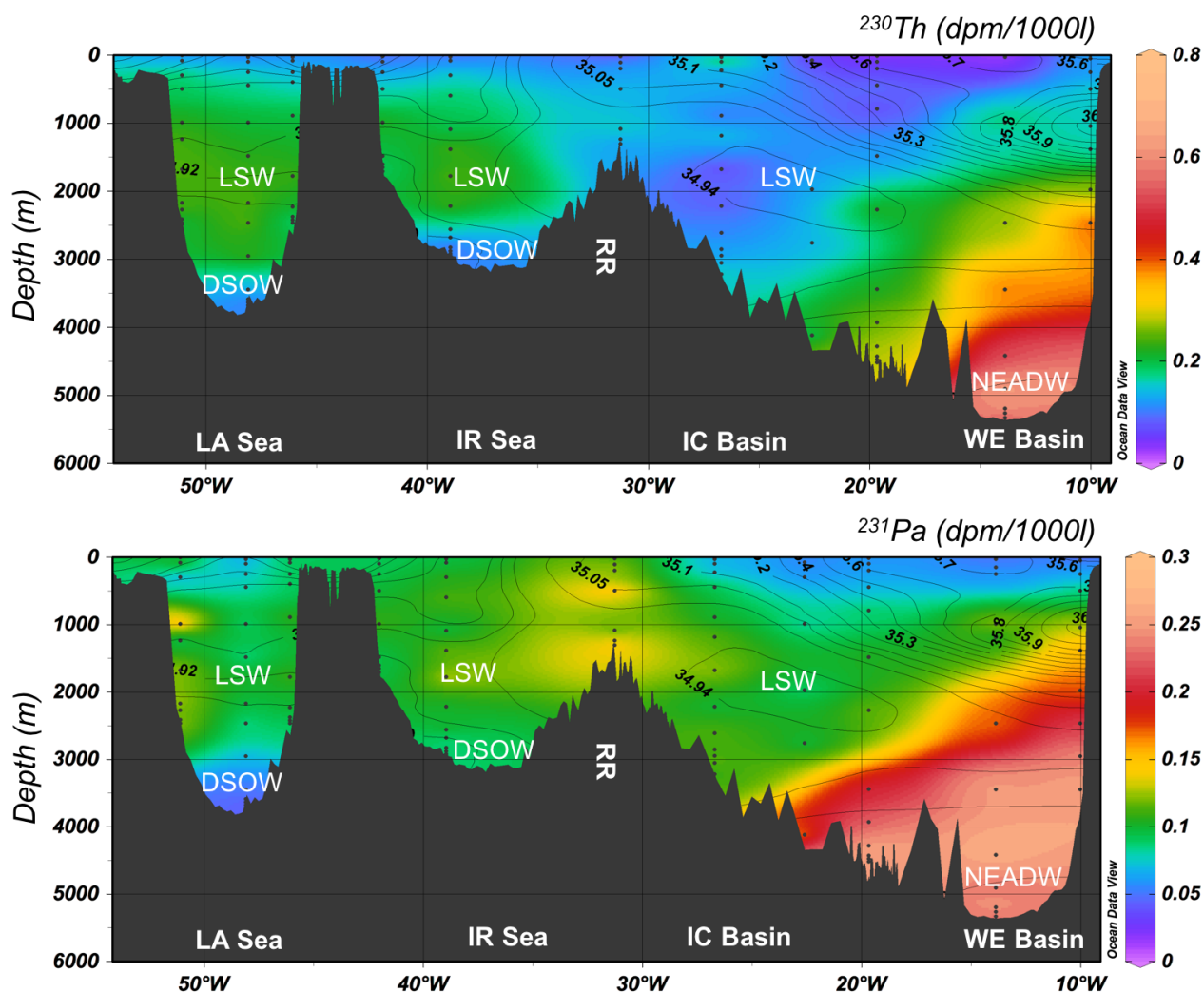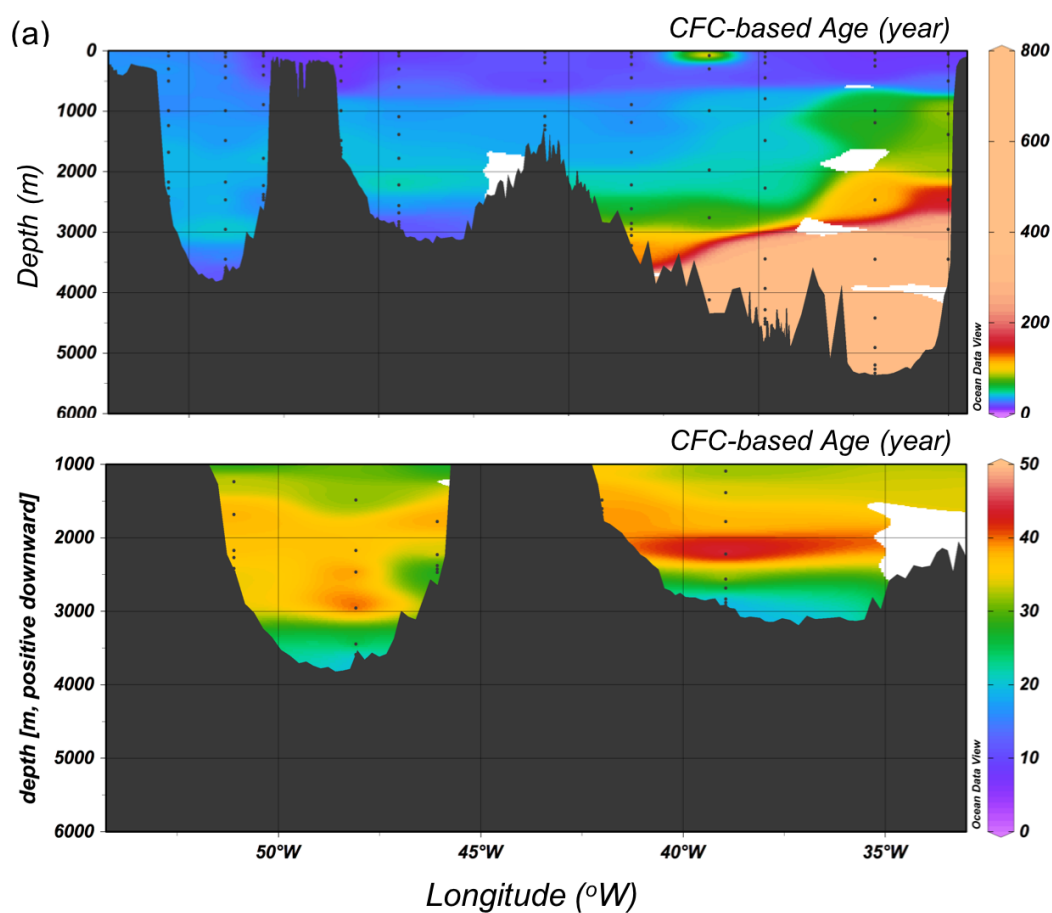**Rise.**

Figure 5: Distribution of ^{230}**Th and** ^{231}**Pa along the GEOVIDE section. Salinity concentrations are also plotted as contours, and water-masses labelled.**

Figure 6: Water mass age based on CFC data along the GEOVIDE section. (a) Full water-column data for the entire section, showing waters from 10 to 800 years in age; (b) A rescaled version of (a) omitting the upper 1000m and the older waters west of 35°W to show age variation in recently ventilated deep-waters.

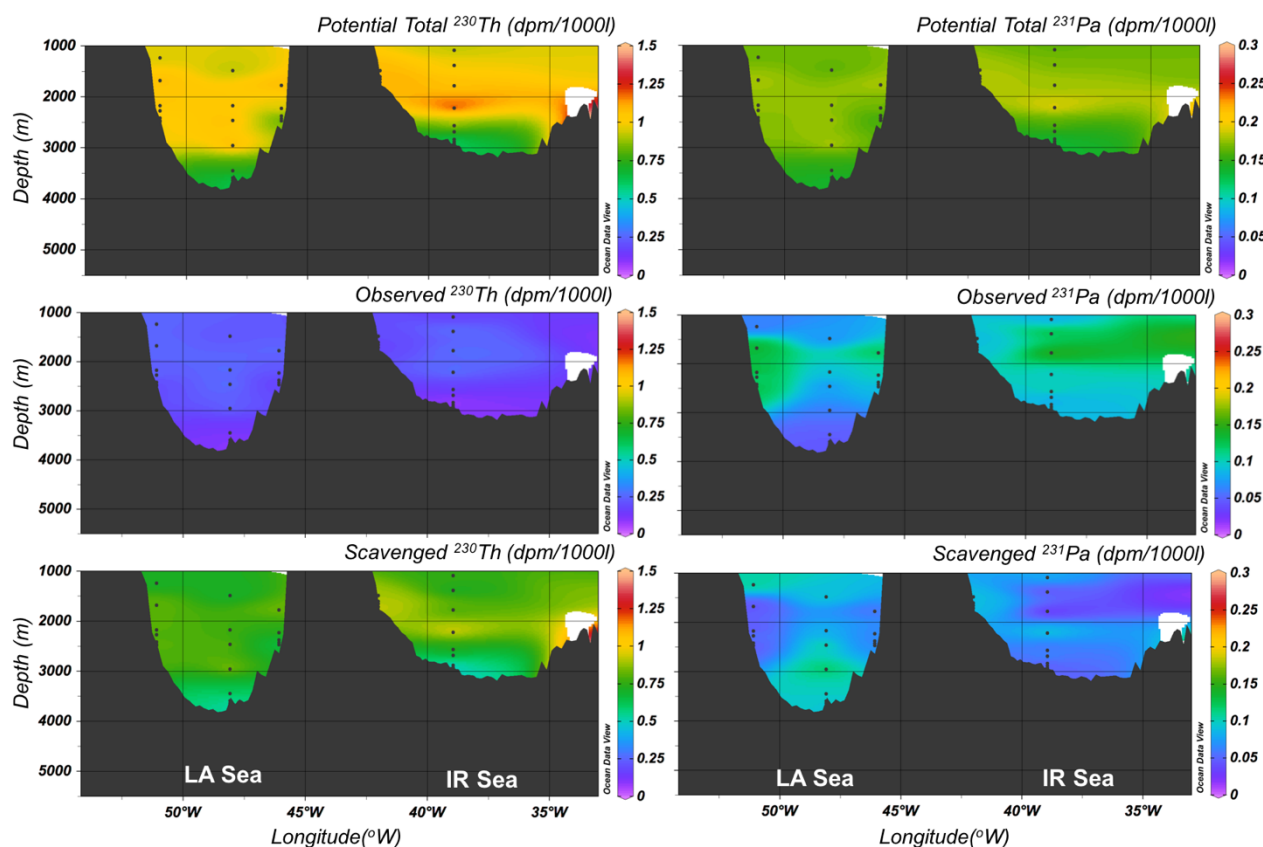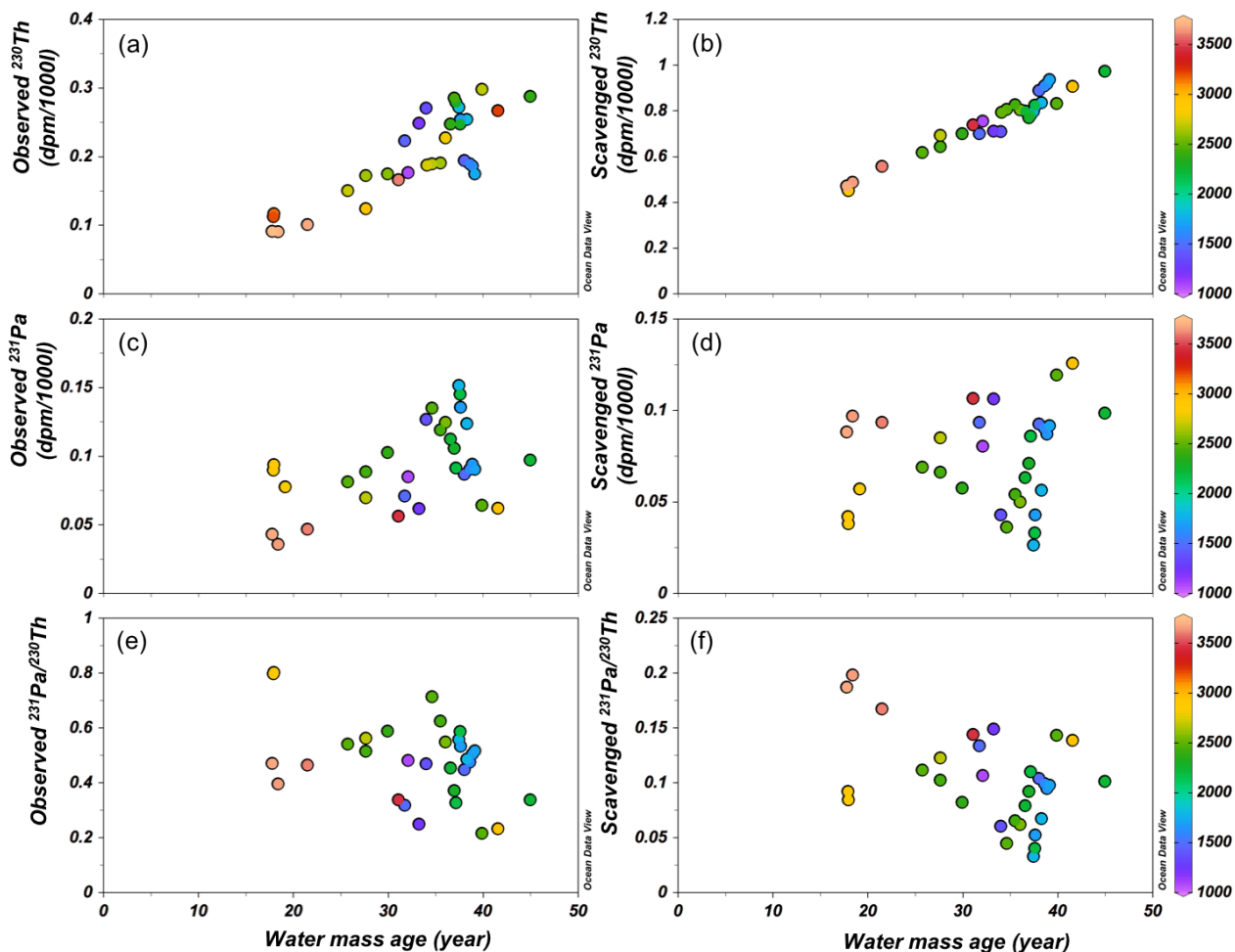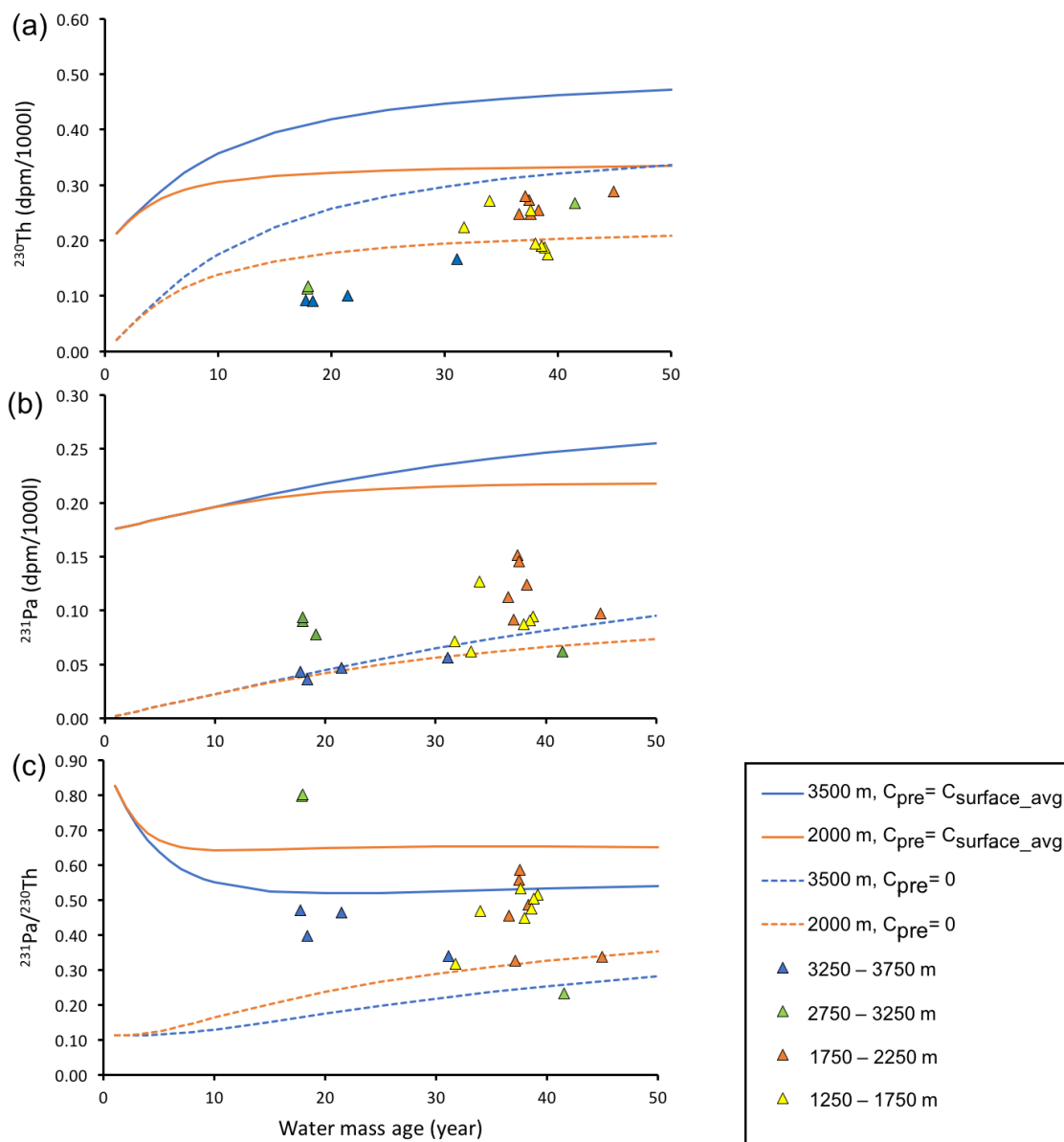**Figure 7: Potential Total, Observed, and Scavenged components of ²³⁰Th and ²³¹Pa in waters >1000 m water depth and west of 35°W.**

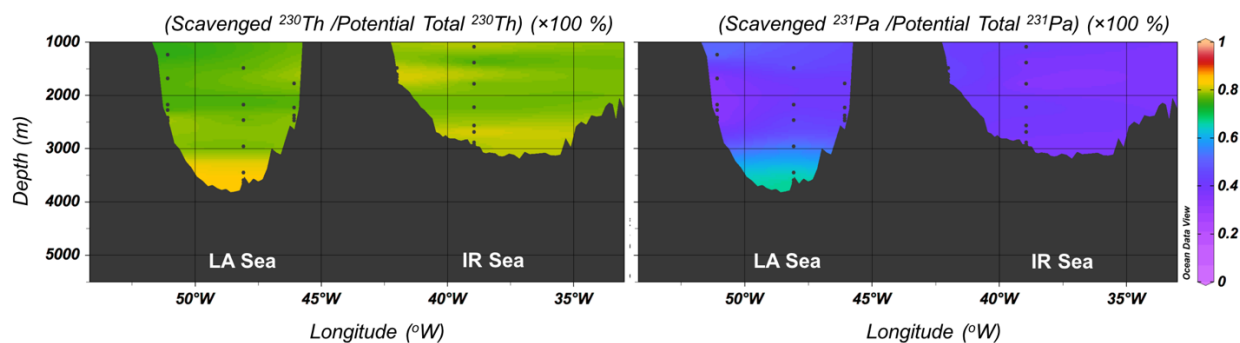**Figure 8: Relationship between water mass age and the Observed and Scavenged components of ^{230}Th, ^{231}Pa and ^{231}Pa/^{230}Th (colour coded by water depth). Note the increase of observed concentrations for both nuclides with age. Comparison of average values indicates that about three quarters of ^{230}Th produced by decay is scavenged, compared with about half of the ^{231}Pa.**

Figure 9: Results from a scavenging-mixing model of ^{230}Th, ^{231}Pa, and ^{231}Pa/^{230}Th compared to observations. Preformed values were set at 0 (dashed line) and at the average surface values from GEOVIDE section (solid line), i.e. ^{230}Th$_{surface}$=0.108 dpm/1000l, ^{231}Pa$_{surface}$=0.089 dpm/1000l.

Figure 10: Ratio of Scavenged component to Potential Total component for ^{230}Th and ^{231}Pa, providing an assessment of the relative importance of scavenging for the two nuclides, and of the location of scavenging.

Figure 11: Fluxes of ^{230}Th (blue arrow) and ^{231}Pa (yellow arrow) across the GEOVIDE section (blue solid line), 4.5°S (green solid line) and 45°S (red solid line). Also shown are production of ^{230}Th (blue box) and ^{231}Pa (yellow box) in the North Atlantic (between GEOVIDE section and 4.5°S) and in the South Atlantic (between 4.5°S and 45°S), based on calculation in Deng et al. (2014). These fluxes indicate that 4% of the ^{230}Th produced in the North Atlantic is exported southward by ocean circulation, and 23% of the ^{231}Pa.